Article

Enzyme-mediated two-step regio- and stereoselective synthesis of potential rapid acting antidepressant (2*S*,6*S*)-hydroxynorketamine

Ansgar Bokel, Ansgar Rühlmann, Michael Christopher Hutter, and Vlada B. Urlacher

ACS Catal., **Just Accepted Manuscript** • DOI: 10.1021/acscatal.9b05384 • Publication Date (Web): 06 Mar 2020

Enzyme-Mediated Two-Step Regio- and Stereoselective Synthesis of Potential Rapid Acting Antidepressant (2*S*,6*S*)-Hydroxynorketamine

Ansgar Bokel,[‡] Ansgar Rühlmann,[‡] Michael C. Hutter,[#] and Vlada B. Urlacher*[,‡]

[‡] Institute of Biochemistry, Heinrich Heine University Düsseldorf, Universitätsstr. 1, 40225 Düsseldorf, Germany

[#] Center for Bioinformatics, Saarland University, Campus E2.1, 66123 Saarbruecken, Germany

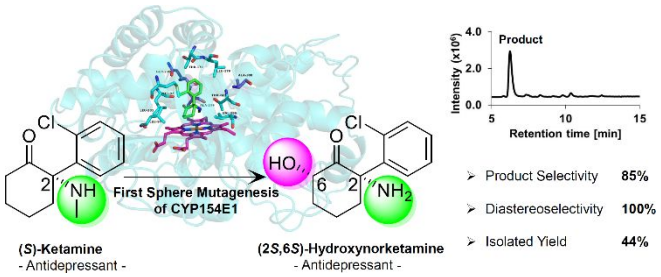

ABSTRACT: Since recently, the anesthetic (*S*)-ketamine has been approved as a rapid-acting and long-lasting antidepressant. Its metabolite (2*S*,6*S*)-hydroxynorketamine has been found to have a similar antidepressant effect but with less undesired side effects of ketamine, which make this compound an interesting target for synthesis. Using first-sphere mutagenesis of the cytochrome P450 154E1 from *Thermobifida fusca* YX we constructed a triple mutant that enables the effective production of (2*S*,6*S*)-hydroxynorketamine from (*S*)-ketamine. This engineered P450 monooxygenase catalyzes the consecutive oxidative *N*-demethylation and highly regio- and stereoselective C6-hydroxylation reactions leading directly to the desired product with 85% product selectivity. The integration of this selective monooxygenase into an *E. coli* whole cell biocatalyst allowed production of (2*S*,6*S*)-hydroxynorketamine at a semi-preparative scale. The metabolite was purified and its structure was confirmed by NMR spectroscopy.

KEYWORDS. Cytochrome P450, protein engineering, ketamine, N-demethylation, hydroxylation, regioselectivity, stereoselectivity

INTRODUCTION

Ketamine, a non-competitive N-methyl-D-aspartate (NMDA) receptor antagonist, was synthesized more than 50 years ago, and since then is widely used as anesthetic agent for the management of acute and chronic pain, often in emergency cases, because of its rapid effect.[1] In the early 2000s ketamine was found to exert unexpected antidepressant effect in patients with treatment-resistant major depression.[2] Major depressive disorder is a common illness that affect more than 300 million people worldwide (about 4% of world population according to the report of World Health Organization, March 2018), and is a major cause for suicidal behaviour.[3] Obviously, there is a demand for efficient antidepressants for the treatment of this disorder. Recent findings demonstrate that ketamine is a promising candidate to meet this demand.[4] This drug has a rapid onset effect often within one hour that is at the same time long-lasting of up to one week.[5] For comparison, currently applied therapeutics need weeks to months until a positive response in patients occurs.[5-6] This high potential of ketamine is underlined by the count of patents secured during the last years.[7]

However, ketamine has a number of side effects like blurred vision, dizziness, dissociation, elevated blood pressure and headache.[8] Moreover, the mechanism of its rapid and long-lasting antidepressant effect remains elusive. Whereas the superior and longer-lasting effect of (*R*)-ketamine has been demonstrated only in animal models, clinical studies are only available for racemic and (*S*)-ketamine so far.[9-11] Interestingly, the therapeutic effect of ketamine lasts up to one week, whereas the half-life of this drug is only 2-3 hours. In humans, ketamine is metabolized by several liver microsomal cytochromes P450. Thereby, the major metabolic pathway follows the *N*-demethylation to form norketamine, which is further oxidized at various positions of the cyclohexanone ring, resulting in hydroxylated norketamine metabolites (Scheme 1, Route A). The reverse reaction order, ketamine hydroxylation followed by *N*-demethylation, was also suggested and leads to the identical metabolites (Scheme 1, Route B).[12-13] Among the identified metabolites, (2*R*,6*R*)-hydroxynorketamine and (2*S*,6*S*)-hydroxynorketamine have attracted particular interest, as they exhibit a longer half-life than ketamine and were recently supposed to be essentially involved in the antidepressant

mechanism or at least support the ketamine activity.[10, 14-15] Since then, the mode of ketamine action has been intensively debated in the literature, and the scientific community seems to be at the very beginning of understanding how the antidepressant effect of ketamine and its metabolites are correlated to each other.

In 2019 (*S*)-ketamine (esketamine) nasal spray (SPRAVATO™) was approved in the U.S. for the therapy of treatment-resistant patients with major depression.[16] This development and the potential of (2*S*,6*S*)-hydroxynorketamine ((2*S*,6*S*)-HNK) as a rapid-onset antidepressant that is devoid of the negative side effects of ketamine,[15] makes this metabolite a target of synthetic approaches. Han et al. reported a chemical route towards (2*S*,6*S*)-HNK starting with 1-o-chlorophenylcyclohexene and resulting in an isolated yield of around 30%.[17] In another chemical synthesis, reported by Zanos et al. the overall yield of (2*S*,6*S*)-HNK synthesis reached 5% when the process was started with racemic norketamine. If the first step - chiral resolution of racemic norketamine with a 9% yield - is not taken into account, the isolated yield reaches 54%. It is important to mention, that in this route demethylation of ketamine was avoided and norketamine was used as starting material.[10]

The shortcomings of the chemical routes to (2*S*,6*S*)-HNK prompted us to seek for a selective enzymatic route starting from (*S*)-ketamine via oxidative *N*-demethylation and C6-hydroxylation. Basically, both C-H bond hydroxylation and *N*-demethylation reactions belong to the repertoire of cytochrome P450 monooxygenases (P450s or CYPs).[18] P450s are heme containing enzymes that catalyze the reductive scission of molecular oxygen. One atom of oxygen is introduced into the substrate molecule, whereas the second oxygen atom is reduced to water. The activation of molecular oxygen occurs via a number of steps that lead to the formation of a reactive heme iron-oxygen complex Fe(IV)=O generally referred to as Compound I.[19-21] Generally, P450 enzymes enable regio-, chemo- and stereospecific oxidations of chemically diverse organic molecules in the presence of NAD(P)H. Among several hepatic P450s involved in ketamine metabolism, the formation of (2*S*,6*S*)-HNK is primarily attributed to CYP2A6 and CYP2B6.[12] The use of those eukaryotic enzymes for the synthesis of (2*S*,6*S*)-HNK is however limited by their low regioselectivity. Along with (2*S*,6*S*)- and (2*R*,6*R*)-HNKs, these human P450s also produce (2*S*,4*S*)-, (2*S*,4*R*)-, (2*S*,5*S*)-, (2*S*,5*R*)-HNK and their respective enantiomers as well as non-demethylated hydroxyketamine products.[12-13, 22]

We focused our attempts on bacterial P450s because they are generally easier to express in recombinant hosts and possess higher activity than their eukaryotic counterparts. Our ultimate goal was to identify and/or engineer a P450 enzyme that enables both *N*-demethylation and C6-hydroxylation of (*S*)-ketamine to directly form the target product (2*S*,6*S*)-HNK. Compound I was suggested to mediate the C-H-bond hydroxylation and *N*-demethylation,[23-24] which suggests that both reactions can be catalyzed by one P450 enzyme at one substrate. However, whereas hydroxylation and *N*-demethylation have been extensively studied, reports describing both reactions catalyzed by one P450 enzyme at the same substrate molecule are rare.

Herein we report the construction, characterization and application of a triple mutant of CYP154E1 from *Thermobifida fusca* YX that enables both the *N*-demethylation and C6-hydroxylation of (*S*)-ketamine with high chemo-, regio- and stereoselectivity, to furnish the desired product (2*S*,6*S*)-HNK.

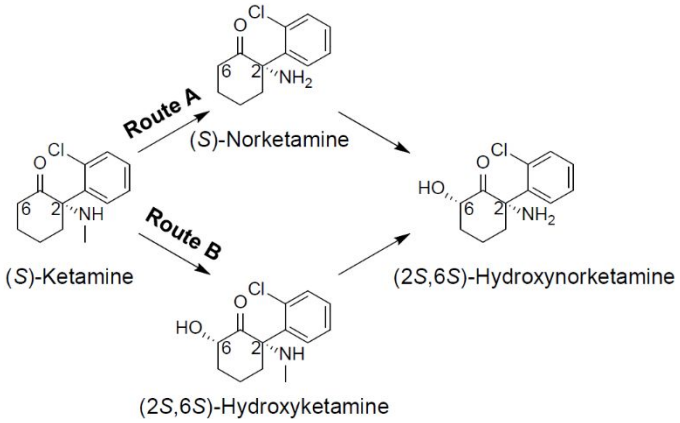

Scheme 1. Oxidation of (*S*)-ketamine to (2*S*,6*S*)-hydroxynorketamine via N-demethylation and hydroxylation at position C6 of the cyclohexanone ring.

RESULTS and DISCUSSION

CYP154E1 mutagenesis

In preliminary experiments, an in-house collection of bacterial cytochrome P450 enzymes and their mutated variants available in our laboratory were tested with (*S*)-ketamine as substrate. CYP154E1 from *Thermobifida fusca* YX, which demonstrated activity towards (*S*)-ketamine, even though resulting in only 2% conversion, was selected for further experiments. This bacterial P450 enzyme is an interesting candidate because it accepts a broad diversity of substrates, possesses high stability, has been used for preparative scale transformations, and its enzymatic properties could be effectively improved by mutagenesis.[25-30] Most P450s rely on NAD(P)H and redox partner proteins for their activity. Since physiological redox partners for CYP154E1 remain unknown, the flavodoxin YkuN from *Bacillus subtilis* and the flavodoxin reductase FdR from *Escherichia coli* were used for electron delivery.[28, 30]

P450 enzymes have been extensively studied and engineered for selective oxidation of diverse substrates for synthetic applications.[31-34] Along with wild type P450s that are capable of regio- and stereoselective oxidations with high activity[35-36] these enzymes were successfully optimized by means of protein engineering. Engineered P450 variants were constructed using directed evolution,[37-38] site-directed mutagenesis,[39-41] site-saturation mutagenesis,[42-44] and combinatorial active-site saturation tests (CAST).[45-46] In our attempt to increase CYP154E1 activity towards (*S*)-ketamine and simultaneously construct a highly selective variant, we applied first-sphere mutagenesis focusing on amino acid substitutions at positions located in a distance of less than 15 Å to the heme iron. First-sphere mutagenesis has been successfully used in our and other research groups to increase activity and selectivity of different P450 enzymes.[27, 47-52] This strategy is based on the hypothesis that positions in the first sphere of the heme iron are likely to interact with any substrate and hence influence its orientation and thereby the regio- and stereoselectivity of the enzyme. Based on a homology model constructed using CYP154A1 from *Streptomyces coelicolor* (PDB 1ODO) as template, and molecular docking of (*S*)-ketamine and (*S*)-norketamine in all possible conformations in the active site of CYP154E1 wild type, we identified 9 first-sphere amino acid residues for mutagenesis (Figures S1).

Several single CYP154E1 mutants with substitutions at the identified positions were already available in our in-house collection (Table S2). Due to the relatively polar nature of ketamine and, common for most P450s rather unpolar CYP154E1 active site, fifteen additional single mutants were constructed with polar amino acids at most identified positions. Especially the positions L235 and I238, located in the I-helix, directly above the heme, seemed appropriate to stabilize the keto- and amino groups of ketamine via hydrogen bonding to the newly introduced polar amino acid residues (Figure S1). Hydrogen bonding between substrate and enzyme can be crucial for determining the selectivity of the P450 as was demonstrated for P450cam (CYP101A1) and P450cin (CYP108).[53] Presence or absence of H-bonds can influence the orientation and stabilization of the substrate in the active site which then alters product formation.[53]

Twenty two out of 25 tested CYP154E1 variants showed similar or lower activity towards (*S*)-ketamine as compared to the wild type enzyme (Figure 1). Only three variants catalyzed oxidation of this substrate with higher activity. Replacement of I238 located in the I-helix above the heme by glutamine resulted in a 12-fold improved substrate conversion. Interestingly, such positive effect was achieved only by introducing a glutamine at position 238. Substitution of I238 with glutamate and asparagine led to complete loss of enzyme activity, which indicates that charged amino acids at this position is strongly disfavored and the length of the side chain does matter as well. Glutamine at position 238 might serve as a hydrogen bond donor for stabilizing (*S*)-ketamine in the orientation, where the amino group is located close to the heme iron, which is not the case in the wild type and might explain the initial low activity (Figure S1).

Another substitution with a pronounced effect on (*S*)-ketamine conversion is G239A. By introducing alanine at position 239, the AGxxT motif conserved among many P450s was reconstituted,[54] which resulted in a 7-fold increased conversion. In our previous study, the G239A substitution in CYP154E1 had a positive effect on stilbene hydroxylation.[27] In the same study again position 238 was in focus of mutagenesis, but because of relatively unpolar stilbene nature, isoleucine at position 238 was replaced by valine.

Substrate conversion was enhanced by a factor of three also by the M388A mutation. The relatively long side chain of methionine lies in a potential substrate binding channel and might hinder the access of (*S*)-ketamine to the heme group.[55] Thus, its removal can be advantageous for heme accessibility for the substrate.

Remarkably, the three best CYP154E1 single mutants I238Q, G239A and M388A did not only demonstrated higher activity, but produced, in contrast to all other variants, hydroxynorketamine in detectable amounts (Figure 2, Table 1 and Table S2). That means that those CYP154E1 variants catalyze both *N*-demethylation and C6-hydroxylation at the same molecule.

In the next step, the mutations I238Q, G239A and M388A were combined to the respective double and triple mutants. Each combination led to higher conversion and regioselectivity for C6-hydroxylation compared to the best single mutant I238Q (Figure 2).

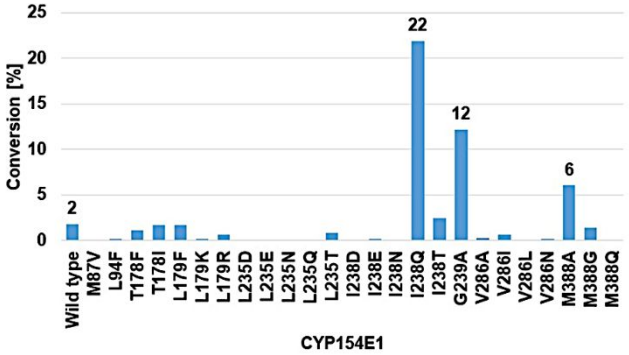

Figure 1. Screening of CYP154E1 mutants with (*S*)-ketamine. Numbers above the bars represent substrate conversion in %. Conversion was calculated by the ratio of the product peaks to the sum of all peak areas. Product analysis was carried out by GC/MS.

Although the M388A single mutant showed only minor improvements compared to the wild type, the integration of this mutation into the double and triple mutants was crucial for high conversion and selectivity. The combination I238Q and M388A drastically increased conversion to 97% (vs. ~ 49% conversion with the single mutant I238Q). In addition, although none of the depicted single mutants exhibited high regioselectivity, the I238Q M388A double mutant produced up to 70% C6-hydroxylated product. Introduction of the G239A mutation in the I238Q M388A double mutant reduced the ratio of undesired products and thus boosted the product selectivity further to above 85%, demonstrated by the triple mutant QAA. Simultaneously, the triple mutant demonstrated the highest activity and caused quantitative conversion of (*S*)-ketamine and of the intermediate (*S*)-norketamine (Figure 2G). Generally, it seems that all three mutations are responsible for the increased selectivity towards (2*S*,6*S*)-HNK.

In attempt to further enhance product selectivity of the QAA variant, T243 was replaced by asparagine, glutamine and serine. Substitutions of this highly conserved threonine located at the distal part of the I-helix in other P450s have influenced various enzyme properties, including regio- and stereoselectivity.[56] Another position selected for mutagenesis was L234, because its substitution was found advantageous for the oxidation of other substrates.[27] None of the constructed quadruple mutants demonstrated higher activity or product selectivity (Figure S2). Thus, the triple CYP154E1 mutant QAA remained the enzyme of choice that demonstrated the highest activity and the highest product selectivity among all constructed CYP154E1 variants.

All CYP154E1 variants listed in Table 1 have in common that they are able to perform both reactions, *N*-demethylation and hydroxylation at the same (*S*)-ketamine molecule to furnish hydroxynorketamine. This capability of performing these two reactions by one P450 enzyme is rather uncommon. *In vitro* studies with a set of hepatic P450s have revealed that *N*-demethylation of ketamine to norketamine was catalyzed with the highest efficiency by CYP2B6, and hydroxylation of norketamine to hydroxynorketamines – by CYP2A6. Although both enzymes were shown to catalyze both reactions, direct conversion of ketamine to hydroxynorketamine(s) with only one of those P450s has not been reported.[12-13] Most studies on drug metabolism including those regarding ketamine metabolism in humans revealed that several P450 enzymes are responsible for hydroxylation and demethylation reactions on the same molecule.[57] Alternatively, one P450 is capable of both reactions but not on the same substrate molecule.[58]

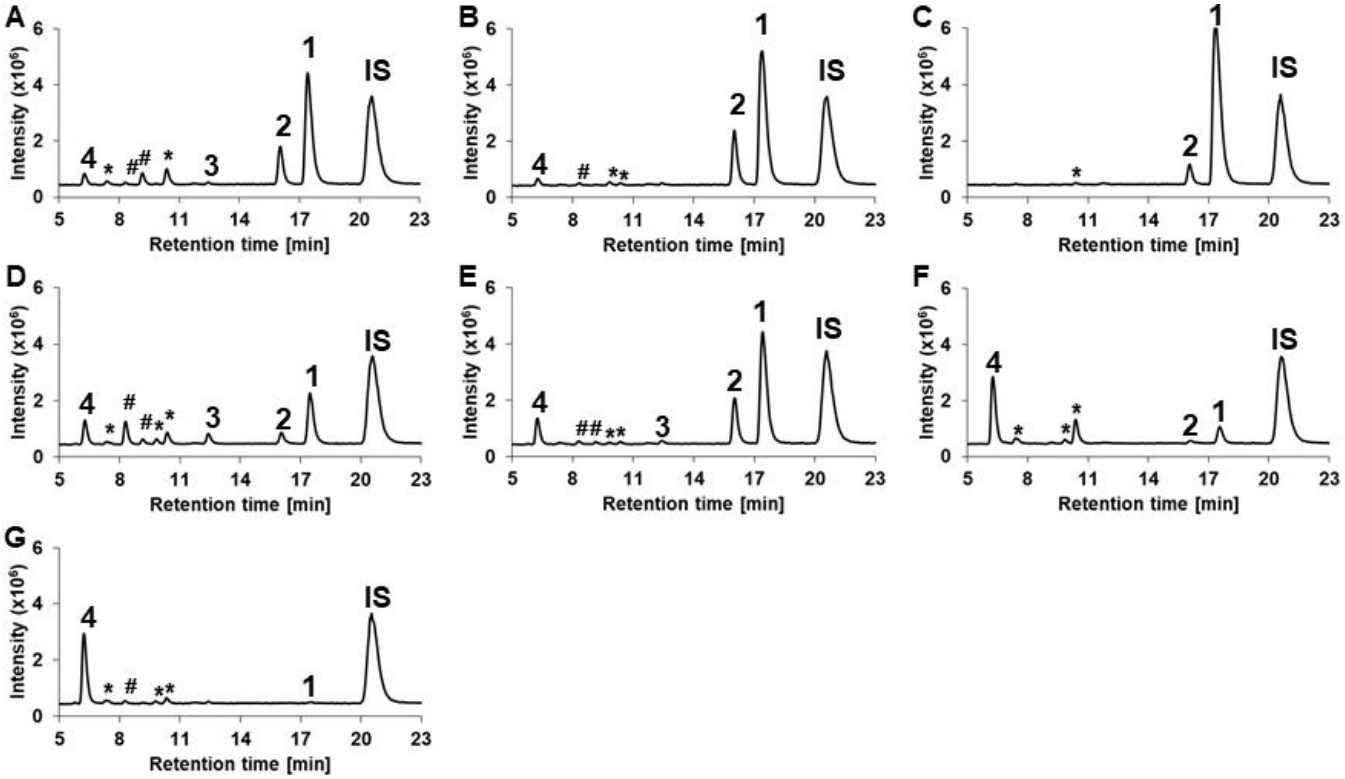

Figure 2. LC/MS chromatograms of (*S*)-ketamine oxidation catalyzed by CYP154E1 I238Q (**A**), G239A (**B**), M388A (**C**), I238Q G239A (**D**), G239A M388A (**E**), I238Q M388A (**F**) and QAA (**G**). IS: xylazine as internal standard, 1: ketamine, 2: norketamine, 3: dehydronorketamine, 4: (2*S*,6*S*)-hydroxynorketamine (identified by comparing with authentic standards, MS fragmentation pattern and NMR analysis), *: unknown hydroxyketamine (assigned by MS fragmentation pattern); #: unknown hydroxynorketamine (assigned by MS fragmentation pattern).

Table 1. (*S*)-ketamine oxidation catalyzed by CYP154E1 variants

		Product distribution [%]					
Mutant	Conv. [%]	NK	DHNK	Rt 8.2 min[a]	Rt 9.1 min[a]	**(2*S*,6)-HNK**	Others[b]
I238Q	49±2	52	2	2	11	**13**	20
G239A	28±3	81	2	2	1	**8**	6
M388A	6±0.5	85	-	1	1	**3**	10
I238Q G239A	85±2	15	11	23	5	**27**	19
G239A M388A	49±4	60	3	3	2	**27**	5
I238Q M388A	97±2	1	-	-	1	**70**	28
I238Q G239A M388A (QAA)	**>99**	**-**	**-**	**3**	**1**	**85**	**11**

NK: norketamine; DHNK: dehydronorketamine; (2*S*,6)-HNK: (2*S*,6)-hydroxynorketamine

[a] products with a retention time of 8.2 and 9.1 min had mass fragmentation equivalent to that of (2*S*,6)-HNK, indicating either configurational or constitutional isomers.

[b] products with mass fragmentation equivalent to that of HK (hydroxyketamine) - hydroxylation but no *N*-demethylation occurred.

Characterization and application of CYP154E1 QAA

Starting with (*S*)-ketamine as substrate, two stereoisomers, namely (2*S*,6*S*)-hydroxynorketamine and its diastereomer (2*S*,6*R*)-hydroxynorketamine can be formed. To better distinguish between the two diastereomers and to analyze the stereoselectivity of CYP154E1 variants during C6-hydroxylation of (*S*)-ketamine, all reactions were analyzed via HPLC on a chiral column (Figure S3). Identification of (2*S*,6*S*)-HNK product occurred via spiking with the authentic (2*S*,6*S*)-HNK standard (Figure S4). Except for (2*S*,6*S*)-hydroxynorketamine no further respective standards were available and the side product formation was too low for the NMR analysis. The chiral HPLC analysis of the QAA-catalyzed (*S*)-ketamine conversion revealed the (2*S*,6*S*)-HNK product peak whose shape is absolutely identical to the peak shape of the authentic standard (Figure S4). This observation indicates a 100% diastereoselectivity of this mutant. Even if one takes all other peaks into consideration, diastereoselectivity would only decrease to 92%.

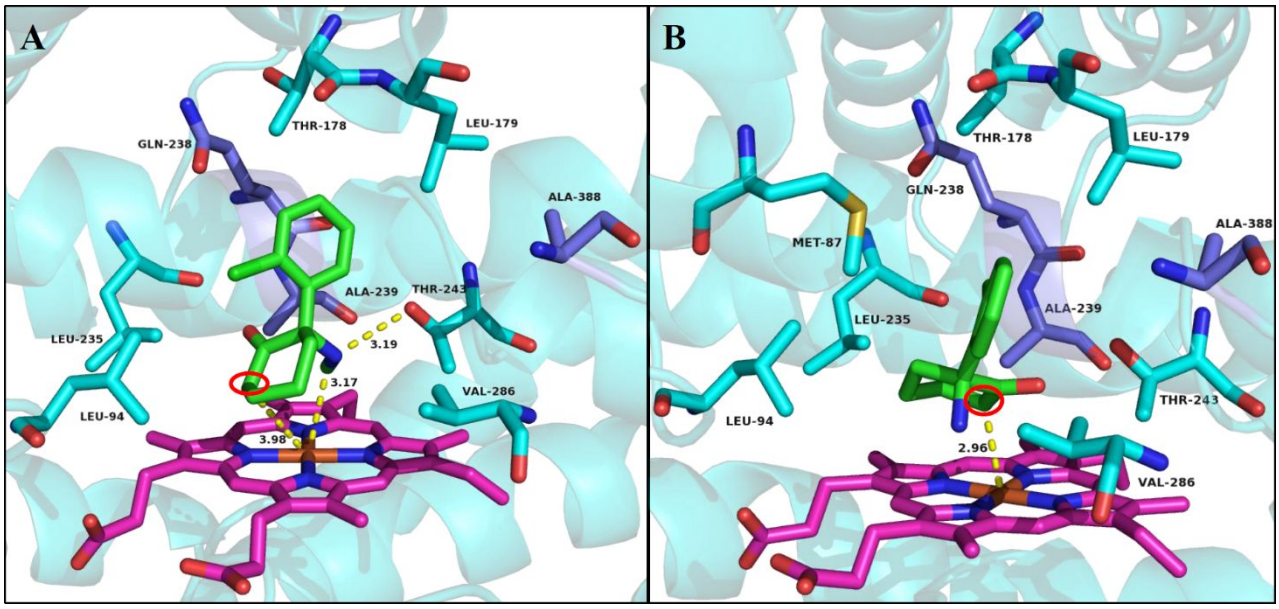

Figure 3. Best scored rigid docking poses of **(S)-ketamine** (green, 3**A**) and **(S)-norketamine** (green, 3**B**) in the active site of CYP154E1 QAA. Position C6 of the cyclohexanone ring is marked by red circle. Dashed yellow lines indicate distances between atoms. The numerical distance is given in Å.

These results were supported by docking studies (Figure 3). The best docking poses of (*S*)-ketamine and (*S*)-norketamine into the active site of CYP154E1 QAA demonstrated that the cyclohexanone ring in both substrates is located above and almost in parallel to the heme group. This position favors the *syn*-attack leading to the highly diastereoselective formation of (2*S*,6*S*)-hydroxynorketamine.

To complete the characterization of the best mutant QAA, the enzyme was purified to homogeneity and characterized regarding substrate binding and reaction kinetics. Upon (*S*)-ketamine titration spectral changes of the Soret band occurred (Figures S5 and S6). The observed Type I-binding spectrum is typical for most P450 substrates. The binding constant K_D of 232 µM is however higher than K_D values estimated for CYP154E1 wild type and other mutants with other reported substrates, such as stilbene, geraniol, nerol and fatty acids.[27-28] Nevertheless, a direct comparison is somewhat questionable, because small changes in the active site of a P450 and in substrate structure might lead to substantial perturbation during binding.

When comparing the kinetic parameters for the CYP154E1 QAA variant (Figure S7) with those found in the literature for human P450s, one recognizes that the K_M of 452±67 µM is in the same order of magnitude as for ketamine oxidizing hepatic P450s.[59] On the other hand, the k_{cat} value of 56.2±4.7 min^{-1} calculated for the QAA variant during (*S*)-ketamine conversion was in all cases higher. For example, the k_{cat} values for the three most active human P450s, CYP2B6, CYP2C9 and CYP3A4 are at least 2-times and up to 6-times lower compared to QAA.[13, 59-60]

Time course studies have revealed that the first detected product of (*S*)-ketamine oxidation was (*S*)-norketamine, whereas (2*S*,6*S*)-HNK appeared later. This finding allowed us to suggest that demethylation and C6-hydroxylation occur in a consecutive manner according to the Route A (Scheme 1), and the overall process is the two-step four electrons oxidation of (*S*)-ketamine. According to substrate docking (Figure 3) the (*S*)-norketamine molecule is rotated about 90° clockwise around the vertical axis as compared to (*S*)-ketamine. This change in orientation brings position C6 1 Å closer to the heme iron (3.0 vs. 4.0 Å for norketamine compared to ketamine) which makes this position more favorable for hydroxylation after demethylation. However, the MS analysis of the side products (Table 1) revealed the presence of low amounts of non-demethylated hydroxyketamine. Even after prolonged reaction times, *N*-demethylation of this hydroxyketamine occurred to a very low extent. Docking of (2*S*,6*S*)-hydroxyketamine (Figure S8) revealed that in this case the amine group of the substrate is located quite far away from the heme iron (7.09 Å), which could explain the observed low demethylation activity of the enzyme towards this metabolite. Thus, the presence of hydroxylated but non-demethylated co-product may be due to a more complex kinetics, which requires further detailed investigations.

For product isolation and testing the applicability of the CYP154E1 QAA variant for (2*S*,6*S*)-HNK production, we increased the reaction volume from 125 µl to 10 ml and the substrate concentrations from 500 µM to 5 mM. This reaction was performed using an *E. coli* based whole-cell biocatalyst harboring the *cyp154E1 QAA* gene and the genes encoding for the heterologous redox partners as described in the experimental section. Within six hours, (*S*)-ketamine HCl at a concentration of up to 1.16 g/L was converted (Figure S9) and (2*S*,6*S*)-hydroxynorketamine at a concentration of 935 mg/L was produced. In comparison to the CYP154E1 QAA, a maximum concentration of 201.6 µg/L (2,6)-HNK produced from the direct precursor (2,6)-hydroxyketamine was achieved in the reaction catalyzed by human CYP2B6. The formation of (2,6)-HNK with other human CYPs was even lower.[12]

The main product was isolated and purified via silica column with an yield of 44% (19.55 mg with 99% purity after conversion of 44.29 mg (*S*)-ketamine) and was confirmed as (2*S*,6*S*)-HNK via spiking experiment with respective standard and NMR analysis (Figure S10-13).

CONCLUSIONS

Ketamine has been recognized as a promising antidepressant for the treatment of major depressive disorder and some other mental diseases. Since 2016, when the antidepressant effect of (2*S*,6*S*)- and (2*R*,6*R*)-hydroxynorketamines was first reported,[10] their mode of action have been steadily discussed in the literature. Very recently, ketamine was suggested to be a prodrug, that is metabolized to hydroxynorketamines with the desired antidepressant effect.[4] In this context, the development of new effective synthetic routes to hydroxynorketamines is of high importance.

Herein, we report a new direct enzymatic route towards (2*S*,6*S*)-hydroxynorketamine. First-sphere mutagenesis at several positions located in close proximity to the heme group of CYP154E1, followed by combining the best mutations, led to the QAA triple mutant that possess high product selectivity. In numbers, conversion was increased from 2% achieved with the wild type, to >99%. The engineered P450 enzyme is able to catalyze both the *N*-demethylation and the C6-hydroxylation reactions in a consecutive manner with high regio- and stereoselectivity leading to the desired product (2*S*,6*S*)-hydroxynorketamine at a ratio of 85%. In combination with the heterologous redox partners YkuN and FdR, this P450 turned out to be very efficient for selective synthesis of (2*S*,6*S*)-hydroxynorketamine not only *in vitro* but also in form of whole-cell biocatalyst. The developed direct enzymatic route provides an efficient alternative to the chemical synthesis developed by Han *et al*. 2017.[17] In the chemical four steps approach an overall yield of around 30% was reached. In our CYP154E1 QAA mediated process starting with (*S*)-ketamine, (2*S*,6*S*)-hydroxynorketamine of 99% purity was formed with an isolated yield of 44%. This P450-catalyzed reaction can further be combined with a simple chemical kinetic resolution of *rac*-ketamine with tartaric acid,[61] which would reduce the overall production costs.

EXPERIMENTAL SECTION

Cloning. Mutagenesis, expression and purification of enzymes are described in the Supporting Information and Table S1.

Docking study: The homology model of CYP154E1 was created using the SWISS-MODEL[62-65] server and the crystal structure of CYP154A1 (PDB: 1ODO) as template. The coordinates of the heme were manually integrated into the homology model. The analysis of the homology model was done as described by Petrović and Zlatović in 2015.[66] The 3D structures of (*S*)-ketamine and (*S*)-norketamine in all stereoisomeric forms were obtained from the Cambridge Structural Database. Rigid docking was performed using Autodock 4.0.[67-70] Parameters files were created using AutoDockTools. Visualization of the results was carried out with PyMOL software.

Oxidation reaction on an analytical scale. All reactions were performed in 100 mM potassium phosphate buffer pH 7.5. Enzyme screening reactions were performed in 125 µl volume using *E. coli* cell lysate at 25°C and 600 rpm. The reaction mixture consisted of 500 µM (*S*)-ketamine (dissolved in water), 2.5 µM P450 (crude cell lysate), 2.5 µM purified FdR, 25 µM purified YkuN and 200 µM NADPH. NADPH recycling was supported by 5 U/ml GDH in the presence of 20 mM glucose. Decomposition of potentially formed hydrogen peroxide, due to P450 uncoupling reactions, was achieved by addition of 600 U/ml catalase. Reactions were stopped after 17 hours by adding 125 µl of 1 M Na_2CO_3. Extraction of the reaction mixtures was done twice with 200 µl ethyl acetate each. The combined organic phases were evaporated to dryness and resolved in 100 µl acetonitrile (for LC/MS analysis) or 100 µl ethanol (for HPLC analysis). Substrate conversion in the screening experiments were based on the ratio between the sum of product peak areas compared to the sum of all peak areas. For all reactions other than the screening, 222 µM xylazine hydrochloride served as an internal standard for quantification and was added directly before the reaction was stopped by addition of 1 M Na_2CO_3.

Oxidation reaction for product isolation. For reaction at higher scale an *in vivo* two-plasmid whole-cell biotransformation system was created. Therefore, the genes of the redox proteins YkuN and FdR were cloned into the first and respectively second multiple cloning site of the pCOLA Duet vector system. The P450 gene was cloned into pET22b as second vector system. Expression was done in autoinduction medium using lactose as inducer once glucose is consumed as preferred carbon source. Overall expression was carried out in 500 ml flasks containing 100 ml medium, initially at 37°C and 180 rpm until OD_{600} of 1.0 was reached. Afterwards cultures were stirred for another 20 hours at 25°C and 120 rpm before cells were harvested. *E. coli* cells were washed once with reaction buffer (containing) and subsequent cell density was adjusted to 50 mg/ml cell density (cell wet weight) in reaction buffer before the suspension was frozen at -80°C for at least 24 hours. (*S*)-ketamine (2 mM of 5 mM final concentration, dissolved in water) was added to 10 ml of thawed *E. coli* cell suspensions (50 mg/ml) and the reaction mixture was incubated in round-bottom flasks at 25°C and 230 rpm. Extraction was done similar to the extraction at analytical scale except that volumes of 1 M Na_2CO_3 and ethyl acetate were adjusted to 1 ml and twice 7.5 ml respectively. Organic layers were combined, dried over $NaSO_4$ and removed under reduced pressure. The main product (2*S*,6*S*)-HNK was isolated with flash chromatography on a silica column using a mobile phase consistent of 60% chloroform, 35% ethyl acetate, 5% methanol and 0.1% ammonium hydroxide. Fractions were first analyzed via TLC using the same mobile phase and those with products were further analyzed via LC/MS and NMR (for details see below).

Product analysis. Screening of CYP154E1 mutant minimal library was carried out via GC/MS on a GC/MS QP-2010 Plus (Shimadzu, Duisburg, Germany) with a FS-Supreme-5ms (30 m x 0.25 mm x 0.25 µm) column and helium as carrier gas. Samples were injected at an injection temperature of 300°C. Starting with a column oven temperature of 170°C held for two minutes, the temperature then increased with the rate of 20°C per minute till 300°C and held again for another four minutes.

LC/MS analysis was performed on LCMS-2020 (Shimadzu) on a Chromolith® Performance RP-8e 100-4.6 mm (Merck Millipore) column, equipped with a Chromolith® RP-8e 5-4.6 mm guard cartridge using xylazine (222 µM concentration) as internal standard. Elution occurred on a gradient between water (supplemented with 0.1% formic acid) and acetonitrile.

Stereoselectivity was analyzed using LC-2020 (Shimadzu) equipped with the chiral column Chiralpak IB (0.46 cm Ø x 25 cm, Chiral Technologies Europe) and an isocratic elution mode consisting of 97% n-hexane and 3% ethanol.

Products and substrates were identified by their retention times and mass fragmentation patterns (GC/MS and LC/MS)

compared to the corresponding values of authentic reference compounds and literature.[71] Conversions were determined either via substrate depletion compared to the negative control or via internal standard quantification using xylazine as internal standard.

Structure elucidation (2*S*,6*S*)-hydroxynorketamine (**4**): ^{1}H NMR (600 MHz, Chloroform-*d*) (Figure S10): δ 7.62 – 7.57 (m, 2H), 7.41 – 7.26 (m, 2H), 4.20 (dd, J = 11.7, 6.9 Hz, 1H), 2.93 – 2.86 (m, 1H), 2.39 – 2.31 (m, 1H), 2.03 (s, 2H), 1.74 – 1.64 (m, 2H), 1.67 – 1.54 (m, 1H), 1.51 – 1.40 (m, 1H). ^{13}C NMR (151 MHz, Chloroform-*d*) (Figure S11): δ 214.65, 138.17, 133.79, 131.58, 129.86, 128.78, 127.78, 73.75, 67.28, 42.19, 40.02, 19.40. Further structure elucidation was done by 2D-NMR (Figures S12 and S13).

Kinetic studies The reaction conditions and mixture were similar to those for the analytical conversions. Instead of cell free lysate purified CYP154E1 QAA at a final concentration of 0.5 µM was used. The concentrations of purified FdR and YkuN were adjusted to 0.5 and 20 µM, respectively. To calculate the kinetic constants, the initial activity of CYP154E1 QAA was monitored at (*S*)-ketamine concentrations ranging from 50 to 2000 µM. The reactions were stopped after 5 to 20 min by addition of 1 M sodium carbonate and xylazine (222 µM) as internal standard. Conversions were analyzed on a LCMS-2020 (as described in product analysis). For calculation of k_{cat} and K_M, the data were fitted according to the equation of Michaelis-Menten by non-linear regression using RStudio software (Figure S7) (RStudio Team (2015). RStudio: Integrated Development for R. RStudio, Inc., Boston, MA URL http://www.rstudio.com/).

Determination of substrate dissociation constant (K_D). Upon substrate binding in the P450 active site spectral changes, related to the changes in the heme iron spin state, were determined using a Lambda 35 double beam UV/VIS spectrometer (Perkin-Elmer, Germany) equipped with two tandem quartz cuvettes (Hellma, Germany). Procedure was done according to Rühlmann et al 2017.[27] 1 µM purified P450 enzyme buffered in 100 mM potassium phosphate buffer pH 7.5 was used. Volumes of 0.5-10 µl of (*S*)-ketamine stock solutions were added successively. For calculation of K_D, the data were fitted according to Michaelis-Menten like hyperbolic equation by non-linear regression using RStudio software (RStudio Team (2015). RStudio: Integrated Development for R. RStudio, Inc., Boston, MA URL http://www.rstudio.com/).

AUTHOR INFORMATION

Corresponding Author

Vlada B. Urlacher - Institute of Biochemistry, Heinrich Heine University Düsseldorf, Universitätsstr. 1, 40225 Düsseldorf, Germany; orcid.org/0000-0003-1312-4574; E-mail: Vlada.Urlacher@uni-duesseldorf.de

Authors

Ansgar Bokel - Institute of Biochemistry, Heinrich Heine University Düsseldorf, Universitätsstr. 1, 40225 Düsseldorf, Germany

Ansgar Rühlmann - Institute of Biochemistry, Heinrich Heine University Düsseldorf, Universitätsstr. 1, 40225 Düsseldorf, Germany

Michael C. Hutter - Center for Bioinformatics, Saarland University, Campus E2.1, 66123 Saarbruecken, Germany

Notes

The authors declare no competing financial interest.

ASSOCIATED CONTENT

Supporting Information

The Supporting Information is available free of charge on the ACS Publications website.

Experimental details, enzyme assays, chromatographic and spectral data, and NMR spectra.

ACKNOWLEDGMENT

We wish to thank Sebastian Hölzel, Heinrich Heine University Düsseldorf, Germany, for technical assistance. Generous financial support by the Federal Ministry of Education and Research to Heinrich Heine University Düsseldorf (grant number 031A223A) is gratefully acknowledged.

REFERENCES

(1) Domino, E. F.; Chodoff, P.; Corssen, G. Pharmacologic Effects of CI-581, a New Dissociative Anesthetic, in Man. *Clin. Pharmacol. Ther.* **1965**, *6*, 279-291.

(2) Berman, R. M.; Cappiello, A.; Anand, A.; Oren, D. A.; Heninger, G. R.; Charney, D. S.; Krystal, J. H. Antidepressant Effects of Ketamine in Depressed Patients. *Biol. Psychiatry* **2000**, *47*, 351-354.

(3) Eikelenboom, M.; Beekman, A. T. F.; Penninx, B. W. J. H.; Smit, J. H. A 6-Year Longitudinal Study of Predictors for Suicide Attempts in Major Depressive Disorder. *Psychol. Med.* **2018**, *49*, 911-921.

(4) Torjesen, I. Ketamine Could Be First of New Generation of Rapid Acting Antidepressants, say Experts. *BMJ* **2019**, *366*, l4714.

(5) Monteggia, L. M.; Zarate, C., Jr. Antidepressant Actions of Ketamine: From Molecular Mechanisms to Clinical Practice. *Curr. Opin. Neurobiol.* **2015**, *30*, 139-143.

(6) Scheuing, L.; Chiu, C.-T.; Liao, H.-M.; Chuang, D.-M. Antidepressant Mechanism of Ketamine: Perspective from Preclinical Studies. *Front. Neurosci.* **2015**, *9*.

(7) 22 Patents from 2006 to 2019 (Google Patents: Search Item: Ketamine or Esketamine; Search Item: Depression or Disorder, accessed October 24, 2019.

(8) Short, B.; Fong, J.; Galvez, V.; Shelker, W.; Loo, C. K. Side-Effects Associated with Ketamine Use in Depression: A Systematic Review. *Lancet Psychiatry* **2018**, *5*, 65-78.

(9) Zanos, P.; Gould, T. D. Intracellular Signaling Pathways Involved in (*S*)- and (*R*)-Ketamine Antidepressant Actions. *Biol. Psychiatry* **2018**, *83*, 2-4.

(10) Zanos, P.; Moaddel, R.; Morris, P. J.; Georgiou, P.; Fischell, J.; Elmer, G. I.; Alkondon, M.; Yuan, P.; Pribut, H. J.; Singh, N. S.; Dossou, K. S.; Fang, Y.; Huang, X. P.; Mayo, C. L.; Wainer, I. W.; Albuquerque, E. X.; Thompson, S. M.; Thomas, C. J.; Zarate, C. A., Jr.; Gould, T. D. NMDAR Inhibition-Independent Antidepressant Actions of Ketamine Metabolites. *Nature* **2016**, *533*, 481-486.

(11) Zhang, J.-C.; Li, S.-X.; Hashimoto, K. *R*-(-)-Ketamine Shows Greater Potency and Longer Lasting Antidepressant Effects Than *S*-(+)-Ketamine. *Pharmacol. Biochem. Behav.* **2014**, *116*, 137-141.

(12) Desta, Z.; Moaddel, R.; Ogburn, E. T.; Xu, C.; Ramamoorthy, A.; Venkata, S. L.; Sanghvi, M.; Goldberg, M. E.; Torjman, M. C.; Wainer, I. W. Stereoselective and Regiospecific Hydroxylation of Ketamine and Norketamine. *Xenobiotica* **2012**, *42*, 1076-1087.

(13) Portmann, S.; Kwan, H. Y.; Theurillat, R.; Schmitz, A.; Mevissen, M.; Thormann, W. Enantioselective Capillary Electrophoresis for Identification and Characterization of Human Cytochrome P450 Enzymes Which Metabolize Ketamine and Norketamine *in Vitro*. *J. Chromatogr. A* **2010**, *1217*, 7942-7948.

(14) Paul, R. K.; Singh, N. S.; Khadeer, M.; Moaddel, R.; Sanghvi, M.; Green, C. E.; O'Loughlin, K.; Torjman, M. C.; Bernier, M.; Wainer, I. W. (*R*,*S*)-Ketamine Metabolites (*R*,*S*)-Norketamine and (2*S*,6*S*)-Hydroxynorketamine Increase the Mammalian Target of Rapamycin Function. *Anesthesiology* **2014**, *121*, 149-159.

(15) Singh, N. S.; Zarate, C. A., Jr.; Moaddel, R.; Bernier, M.; Wainer, I. W. What Is Hydroxynorketamine and What Can It Bring to Neurotherapeutics? *Expert Rev. Neurother.* **2014**, *14*, 1239-1242.

(16) Johnson + Johnson Janssen Submits European Marketing Authorisation Application for Esketamine Nasal Spray for Treatment-Resistant Depression. https://www.jnj.com/janssen-submits-european-marketing-authorisation-application-for-esketamine-nasal-spray-for-treatment-resistant-depression, accessed October 22, 2019.

(17) Han, Y.; Mahender Reddy, K.; Corey, E. J. Simple Enantioselective Syntheses of (2*R*,6*R*)-Hydroxynorketamine and Related Potential Rapid-Onset Antidepressants. *Org. Lett.* **2017**, *19*, 5224-5227.

(18) Bernhardt, R.; Urlacher, V. B. Cytochromes P450 as Promising Catalysts for Biotechnological Application: Chances and Limitations. *Appl. Microbiol. Biotechnol.* **2014**, *98*, 6185-6203.

(19) Rittle, J.; Green, M. T. Cytochrome P450 Compound I: Capture, Characterization, and C-H Bond Activation Kinetics. *Science* **2010**, *330*, 933-937.

(20) Grant, J. L.; Hsieh, C. H.; Makris, T. M. Decarboxylation of Fatty Acids to Terminal Alkenes by Cytochrome P450 Compound I. *J. Am. Chem. Soc.* **2015**, *137*, 4940-4943.

(21) Groves, J. T.; Subramanian, D. V. Hydroxylation by Cytochrome-P-450 and Metalloporphyrin Models - Evidence for Allylic Rearrangement. *J. Am. Chem. Soc.* **1984**, *106*, 2177-2181.

(22) Moaddel, R.; Venkata, S. L.; Tanga, M. J.; Bupp, J. E.; Green, C. E.; Iyer, L.; Furimsky, A.; Goldberg, M. E.; Torjman, M. C.; Wainer, I. W. A Parallel Chiral-Achiral Liquid Chromatographic Method for the Determination of the Stereoisomers of Ketamine and Ketamine Metabolites in the Plasma and Urine of Patients with Complex Regional Pain Syndrome. *Talanta* **2010**, *82*, 1892-1904.

(23) Karki, S. B.; Dinnocenzo, J. P.; Jones, J. P.; Korzekwa, K. R. Mechanism of Oxidative Aminedealkylation of Substituted N,N-Dimethylanilines by Cytochrome P450 - Application of Isotope Effect Profiles. *J. Am. Chem. Soc.* **1995**, *117*, 3657-3657.

(24) Dubey, K. D.; Wang, B.; Vajpai, M.; Shaik, S. MD Simulations and QM/MM Calculations Show that Single-Site Mutations of Cytochrome P450 BM3 Alter the Active Site's Complexity and the Chemoselectivity of Oxidation without Changing the Active Species. *Chem. Sci.* **2017**, *8*, 5335-5344.

(25) Bogazkaya, A. M.; von Buhler, C. J.; Kriening, S.; Busch, A.; Seifert, A.; Pleiss, J.; Laschat, S.; Urlacher, V. B. Selective Allylic Hydroxylation of Acyclic Terpenoids by CYP154E1 from *Thermobifida fusca* YX. *Beilstein J. Org. Chem.* **2014**, *10*, 1347-1353.

(26) Hernandez-Martin, A.; von Buhler, C. J.; Tieves, F.; Fernandez, S.; Ferrero, M.; Urlacher, V. B. Whole-Cell Biotransformation with Recombinant Cytochrome P450 for the Selective Oxidation of Grundmann's Ketone. *Bioorg. Med. Chem.* **2014**, *22*, 5586-5592.

(27) Rühlmann, A.; Antovic, D.; Müller, T. J. J.; Urlacher, V. B. Regioselective Hydroxylation of Stilbenes by Engineered Cytochrome P450 from *Thermobifida fusca* YX. *Adv. Synth. Catal.* **2017**, *359*, 984-994.

(28) von Bühler, C. J; Le-Huu, P.; Urlacher, V. B. Cluster Screening: An Effective Approach for Probing the Substrate Space of Uncharacterized Cytochrome P450s. *ChemBioChem* **2013**, *14*, 2189-2198.

(29) von Bühler, C. J.; Urlacher, V. B. A Novel P450-Based Biocatalyst for the Selective Production of Chiral 2-Alkanols. *Chem. Commun.* **2014**, *50*, 4089-4091.

(30) Tieves, F.; Erenburg, I. N.; Mahmoud, O.; Urlacher, V. B. Synthesis of Chiral 2-Alkanols from *n*-Alkanes by a *P. putida* Whole-Cell Biocatalyst. *Biotechnol. Bioeng.* **2016**, *113*, 1845-1852.

(31) Girvan, H. M.; Munro, A. W. Applications of Microbial Cytochrome P450 Enzymes in Biotechnology and Synthetic Biology. *Curr. Opin. Chem. Biol.* **2016**, *31*, 136-145.

(32) Wei, Y.; Ang, E. L.; Zhao, H. Recent Developments in the Application of P450 Based Biocatalysts. *Curr. Opin. Chem. Biol.* **2018**, *43*, 1-7.

(33) Urlacher, V. B.; Girhard, M. Cytochrome P450 Monooxygenases in Biotechnology and Synthetic Biology. *Trends Biotechnol.* **2019**, *37*, 882-897.

(34) Zhang, R. K.; Huang, X.; Arnold, F. H. Selective CH Bond Functionalization with Engineered Heme Proteins: New Tools to Generate Complexity. *Curr. Opin. Chem. Biol.* **2019**, *49*, 67-75.

(35) Manning, J.; Tavanti, M.; Porter, J. L.; Kress, N.; De Visser, S. P.; Turner, N. J.; Flitsch, S. L. Regio- and Enantio-Selective Chemo-Enzymatic C-H-Lactonization of Decanoic Acid to (*S*)-δ-Decalactone. *Angew. Chem. Int. Ed. Engl.* **2019**, *58*, 5668-5671.

(36) Matthews, S.; Tee, K. L.; Rattray, N. J.; McLean, K. J.; Leys, D.; Parker, D. A.; Blankley, R. T.; Munro, A. W. Production of Alkenes and Novel Secondary Products by P450 OleTJE Using Novel H_2O_2-Generating Fusion Protein Systems. *FEBS Lett.* **2017**, *591*, 737-750.

(37) Gillam, E. M. Engineering Cytochrome P450 Enzymes. *Chem. Res. Toxicol.* **2008**, *21*, 220-231.

(38) Jung, S. T.; Lauchli, R.; Arnold, F. H. Cytochrome P450: Taming a Wild Type Enzyme. *Curr. Opin. Biotechnol.* **2011**, *22*, 809-817.

(39) Li, Q. S.; Ogawa, J.; Schmid, R. D.; Shimizu, S. Engineering Cytochrome P450 BM-3 for Oxidation of Polycyclic Aromatic Hydrocarbons. *Appl. Environ. Microbiol.* **2001**, *67*, 5735-5739.

(40) Ost, T. W.; Miles, C. S.; Murdoch, J.; Cheung, Y.; Reid, G. A.; Chapman, S. K.; Munro, A. W. Rational Re-Design of the Substrate Binding Site of Flavocytochrome P450 BM3. *FEBS Lett.* **2000**, *486*, 173-177.

(41) Xu, F.; Bell, S. G.; Rao, Z.; Wong, L. L. Structure-Activity Correlations in Pentachlorobenzene Oxidation by Engineered Cytochrome P450cam. *Protein Eng. Des. Sel.* **2007**, *20*, 473-480.

(42) Denning, A.; Weingartner, A. M.; Kardashliev, T.; Müller, C. A.; Tassano, E.; Schürmann, M.; Ruff, A. J.; Schwaneberg, U. An Enzymatic Route to A-Tocopherol Synthons: Aromatic Hydroxylation of Pseudocumene and Mesitylene with P450 BM3. *Chem.Eur.J.* **2017**, *23*, 17981-17991.

(43) Holec, C.; Hartrampf, U.; Neufeld, K.; Pietruszka, J. P450 BM3-Catalyzed Regio- and Stereoselective Hydroxylation Aiming at the Synthesis of Phthalides and Isocoumarins. *ChemBioChem* **2017**, *18*, 676-684.

(44) Wang, S.; Liu, Z. Oxygenation Cascade Analysis in Conversion of n-Octane Catalyzed by Cytochrome P450 CYP102A3 Mutants at the P331 Site. *Biotechnol. Appl. Biochem.* **2017**, *64*, 14-19.

(45) Acevedo-Rocha, C. G.; Gamble, C. G.; Lonsdale, R.; Li, A. T.; Nett, N.; Hoebenreich, S.; Lingnau, J. B.; Wirtz, C.; Fares, C.; Hinrichs, H.; Deege, A.; Mulholland, A. J.; Nov, Y.; Leys, D.; McLean, K. J.; Munro, A. W.; Reetz, M. T. P450-Catalyzed Regio- and Diastereoselective Steroid Hydroxylation: Efficient Directed Evolution Enabled by Mutability Landscaping. *ACS Catal.* **2018**, *8*, 3395-3410.

(46) Kille, S.; Zilly, F. E.; Acevedo, J. P.; Reetz, M. T. Regio- and Stereoselectivity of P450-Catalysed Hydroxylation of Steroids Controlled by Laboratory Evolution. *Nat. Chem.* **2011**, *3*, 738-743.

(47) Kolev, J. N.; O'Dwyer, K. M.; Jordan, C. T.; Fasan, R. Discovery of Potent Parthenolide-Based Antileukemic Agents Enabled by Late-Stage P450-Mediated C-H Functionalization. *ACS Chem. Biol.* **2014**, *9*, 164-173.

(48) Le-Huu, P.; Petrović, D.; Strodel, B.; Urlacher, V. B. One-Pot Two-Step Hydroxylation of the Macrocyclic Diterpenoid β-Cembrenediol Catalyzed by P450 BM3 Mutants. *ChemCatChem* **2016**, *8*, 3755-3761.

(49) Zhang, K.; Shafer, B. M.; Demars II, M. D.; Stern, H. A.; Fasan, R. Controlled Oxidation of Remote sp^3 C-H Bonds in Artemisinin Via P450 Catalysts with Fine-Tuned Regio- and Stereoselectivity. *J. Am. Chem. Soc.* **2012**, *134*, 18695-18704.

(50) Li, Y.; Wong, L. L. Multi-Functional Oxidase Activity of CYP102A1 (P450BM3) in the Oxidation of Quinolines and Tetrahydroquinolines. *Angew. Chem. Int. Ed. Engl.* **2019**, *58*, 9551-9555.

(51) O'Hanlon, J. A.; Ren, X. K.; Morris, M.; Wong, L. L.; Robertson, J. Hydroxylation of Anilides by Engineered Cytochrome P450(BM3). *Org. Biomol. Chem.* **2017**, *15*, 8780-8787.

(52) Seifert, A.; Antonovici, M.; Hauer, B.; Pleiss, J. An Efficient Route to Selective Bio-Oxidation Catalysts: An Iterative Approach Comprising Modeling, Diversification, and Screening, Based on CYP102A1. *ChemBioChem* **2011**, *12*, 1346-1351.

(53) Slessor, K. E.; Stok, J. E.; Chow, S.; De Voss, J. J. Significance of Protein-Substrate Hydrogen Bonding for the Selectivity of P450-Catalysed Oxidations. *Chem. Eur. J.* **2019**, *25*, 4149-4155.

(54) Mestres, J. Structure Conservation in Cytochromes P450. *Proteins* **2005**, *58*, 596-609.

(55) Wade, R. C.; Winn, P. J.; Schlichting, I.; Sudarko A Survey of Active Site Access Channels in Cytochromes P450. *J. Inorg. Biochem.* **2004**, *98*, 1175-1182.

(56) Clark, J. P.; Miles, C. S.; Mowat, C. G.; Walkinshaw, M. D.; Reid, G. A.; Daff, S. N.; Chapman, S. K. The Role of Thr268 and Phe393 in Cytochrome P450 BM3. *J. Inorg. Biochem.* **2006**, *100*, 1075-1090.

(57) Jiang, Z.-P.; Shu, Y.; Chen, X.-P.; Huang, S.-L.; Zhu, R.-H.; Wang, W.; He, N.; Zhou, H.-H. The Role of CYP2C19 in Amitriptyline *N*-Demethylation in Chinese Subjects. *Eur. J. Clin. Pharmacol.* **2002**, *58*, 109-113.

(58) Olesen, O. V.; Linnet, K. Hydroxylation and Demethylation of the Tricyclic Antidepressant Nortriptyline by cDNA-Expressed Human Cytochrome P-450 Isozymes. *Drug Metab. Dispos.* **1997**, *25*, 740-744.

(59) Hijazi, Y.; Boulieu, R. Contribution of CYP3A4, CYP2B6, and CYP2C9 Isoforms to *N*-Demethylation of Ketamine in Human Liver Microsomes. *Drug Metab. Dispos.* **2002**, *30*, 853-858.

(60) Yanagihara, Y.; Kariya, S.; Ohtani, M.; Uchino, K.; Aoyama, T.; Yamamura, Y.; Iga, T. Involvement of CYP2B6 in *N*-Demethylation of Ketamine in Human Liver Microsomes. *Drug Metab. Dispos.* **2001**, *29*, 887-890.

(61) Steiner, K.; Gangkofner, S.; Grunenwald, J.-M. Racemic Separation of Ketamine. 6,040,479, March 31, 2000.

(62) Arnold, K.; Bordoli, L.; Kopp, J.; Schwede, T. The SWISS-MODEL Workspace: A Web-Based Environment for Protein Structure Homology Modelling. *Bioinformatics* **2006**, *22*, 195-201.

(63) Biasini, M.; Bienert, S.; Waterhouse, A.; Arnold, K.; Studer, G.; Schmidt, T.; Kiefer, F.; Gallo Cassarino, T.; Bertoni, M.; Bordoli, L.; Schwede, T. SWISS-MODEL: Modelling Protein Tertiary and Quaternary Structure Using Evolutionary Information. *Nucleic Acids Res.* **2014**, *42*, W252-W258.

(64) Guex, N.; Peitsch, M. C.; Schwede, T. Automated Comparative Protein Structure Modeling with SWISS-MODEL and Swiss-PdbViewer: A Historical Perspective. *Electrophoresis* **2009**, *30*, S162-S173.

(65) Kiefer, F.; Arnold, K.; Kunzli, M.; Bordoli, L.; Schwede, T. The SWISS-MODEL Repository and Associated Resources. *Nucleic Acids Res.* **2009**, *37*, D387-D392.

(66) Petrović, D.; Zlatović, M. Modeling Human Serum Albumin Tertiary Structure to Teach Upper-Division Chemistry Students Bioinformatics and Homology Modeling Basics. *J. Chem. Educ.* **2015**, *92*, 1233-1237.

(67) Goodsell, D. S.; Olson, A. J. Automated Docking of Substrates to Proteins by Simulated Annealing. *Proteins* **1990**, *8*, 195-202.

(68) Morris, G. M.; Goodsell, D. S.; Halliday, R. S.; Huey, R.; Hart, W. E.; Belew, R. K.; Olson, A. J. Automated Docking Using a Lamarckian Genetic Algorithm and an Empirical Binding Free Energy Function. *J. Comput. Chem.* **1998**, *19*, 1639-1662.

(69) Morris, G. M.; Goodsell, D. S.; Huey, R.; Olson, A. J. Distributed Automated Docking of Flexible Ligands to Proteins: Parallel Application of AutoDock 2.4. *J. Comput.-Aided Mol. Des.* **1996**, *10*, 293-304.

(70) Morris, G. M.; Huey, R.; Lindstrom, W.; Sanner, M. F.; Belew, R. K.; Goodsell, D. S.; Olson, A. J. AutoDock4 and AutoDockTools4: Automated Docking with Selective Receptor Flexibility. *J. Comput. Chem.* **2009**, *30*, 2785-2791.

(71) Wu, C. H.; Huang, M. H.; Wang, S. M.; Lin, C. C.; Liu, R. H. Gas Chromatography-Mass Spectrometry Analysis of Ketamine and Its Metabolites–a Comparative Study on the Utilization of Different Derivatization Groups. *J. Chromatogr. A* **2007**, *1157*, 336-351.

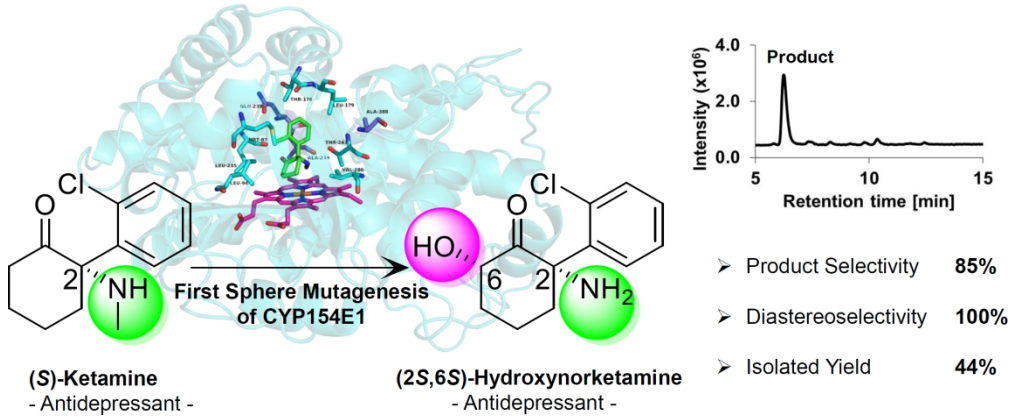

TOC graphic

212x87mm (300 x 300 DPI)

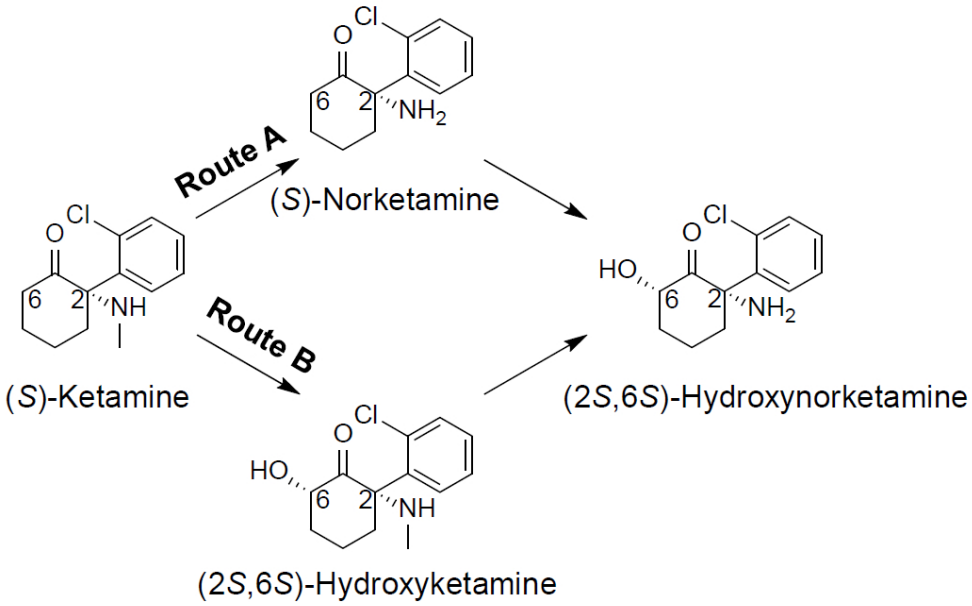

Scheme 1

89x54mm (300 x 300 DPI)

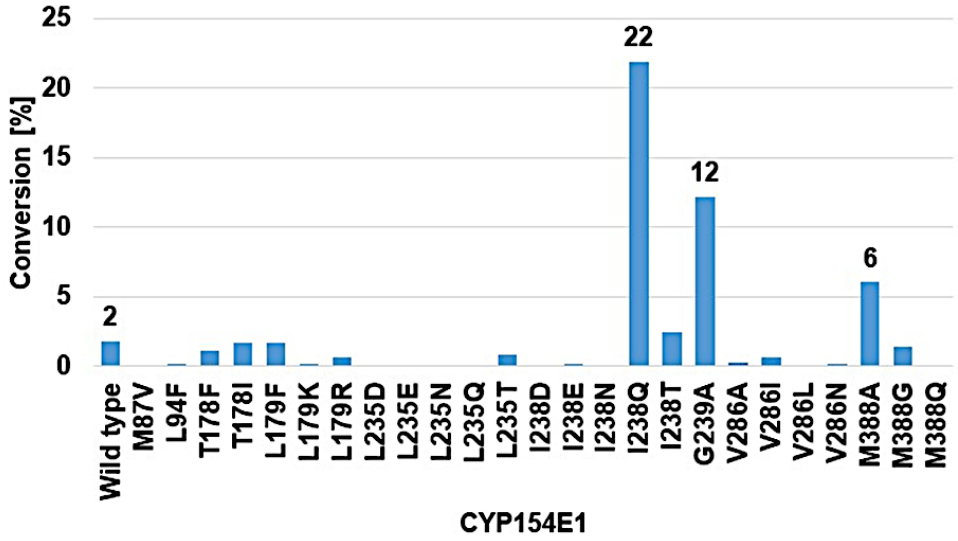

Figure 1

333x190mm (72 x 72 DPI)

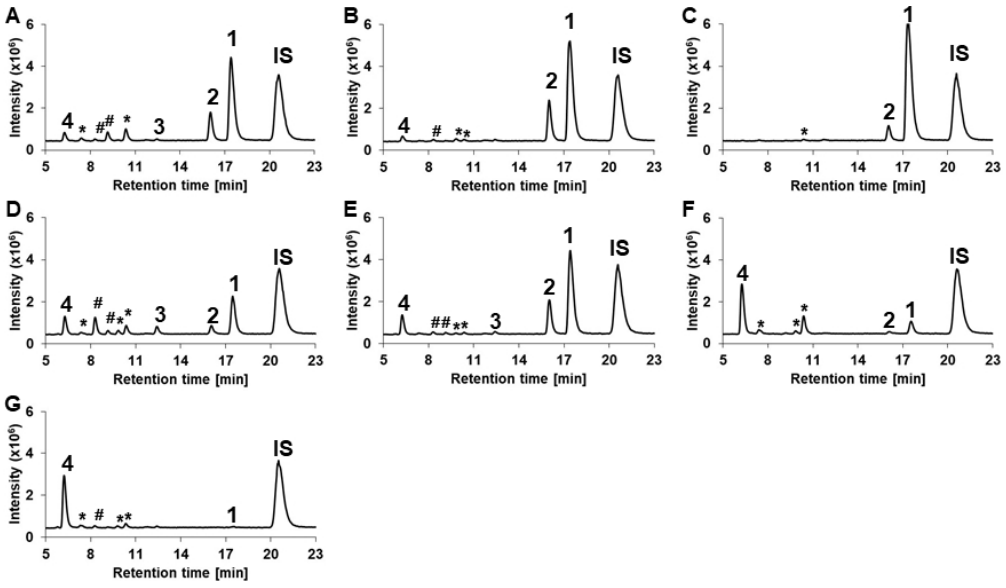

Figure 2

73x42mm (300 x 300 DPI)

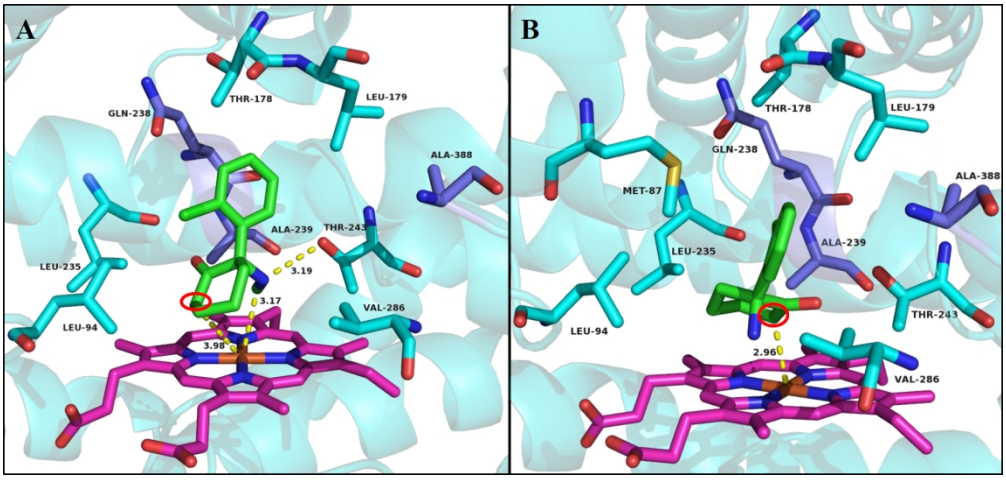

Figure 3

160x75mm (300 x 300 DPI)